

## Multiple Bonding in Four-Coordinated Titanium(IV) Compounds

J. A. Dobado and José Molina Molina\*

Grupo de Modelización y Diseño Molecular, Instituto de Biotecnología, Campus Fuentenueva, Universidad de Granada, 18071 Granada, Spain

Rolf Uggla and Markku R. Sundberg\*

Laboratory of Inorganic Chemistry, Department of Chemistry, P.O. Box 55, A. I. Virtasen aukio 1, FIN-00014 Helsinki, Finland

Received January 5, 2000

Theoretical description (MP2/6-311G\* and B3LYP/6-311G\*) is presented for hypovalent titanium alkoxide model compounds showing linear  $\angle\text{Ti}-\text{O}-\text{C}$  angles. This feature is explained by the existence of a polarized triple Ti–O bond. In contrast, a series of 18 electron germanium derivatives displaying bent  $\angle\text{Ge}-\text{O}-\text{C}$  angles contain polarized single Ge–O bonds. The nature of the Ti–O and Ge–O bonds is established by means of natural bond order, atoms-in-molecules theory, and electron localization function analyses.

### Introduction

Although Hückel's description<sup>1</sup> of a triple bond as consisting of a single  $\sigma$  and two  $\pi$  bonds is still favored, particularly in organic chemistry, it has been challenged since the beginning. The Pauling–Slater concept<sup>2,3</sup> of bent bonds was originally intended to describe double bonds in ethylene, but later Pauling<sup>4</sup> extended the idea to triple bonds.

Although the Hückel concept has traditionally had a hegemony especially in organic chemistry,<sup>5,6</sup> the rivaling model of Pauling and Slater has found some use in describing terminal P–O bonding (sometimes called banana or  $\Omega$  bonding). However, our recent results show clearly that this concept is not adequate to describe the phosphoryl bond.<sup>7</sup>

Computational methods have been used to make the distinction between the two models. Although it was claimed that the traditional Hückel description would be favored over the bent-bond model, some recent quantum chemical calculations strongly support the idea of bent bonds.<sup>8,9</sup>

The traditional description of a multiple bond between a metal and a ligand atom relies on the Hückel concept. These bonds have mostly been found in higher oxidation states of metals, with electron counts of  $d^0$ ,  $d^1$ , and  $d^2$ . Low numbers of the d electrons are needed to provide empty d orbitals for bonding with filled p orbitals of the ligand atoms. Another possibility for the formation of a metal–ligand multiple bond is the donation of metal d electrons to empty ligand atom p orbitals,

as was found for a series of ternary and quaternary metal nitrides.<sup>10</sup>

In their recent study, using natural bond order (NBO) methods to analyze Mo–P and W–P triple bonds in phosphido complexes, Wagener and Frenking<sup>11</sup> demonstrated that the s and p components are not very polarized to either the metal or the phosphorus end.

Application of the atoms-in-molecules (AIM) theory<sup>12–14</sup> has attracted great attention regarding the bonding nature, including the description of possible hypervalent compounds<sup>15–17</sup> and transition metal complexes.<sup>18–22</sup> In this context, Frenking et al.<sup>23,24</sup> revised the concept of the chemical bond to a transition metal by theoretical methods. Multiple bonding to transition metals has recently generated noticeable interest and discussion, including Ga and Al multiple bonding.<sup>25–27</sup> In addition, very

- (10) King, R. B. *Can. J. Chem.* **1995**, *75*, 963.
- (11) Wagener, T.; Frenking, G. *Inorg. Chem.* **1998**, *37*, 1805.
- (12) Bader, R. F. W. *Atoms in Molecules: A Quantum Theory*; Clarendon Press: Oxford, U.K., 1990.
- (13) Bader, R. F. W. *Chem. Rev.* **1991**, *91*, 893.
- (14) See: [www.chemistry.mcmaster.ca/faculty/bader/aim](http://www.chemistry.mcmaster.ca/faculty/bader/aim).
- (15) Dobado, J. A.; Martínez-García, H.; Molina, J.; Sundberg, M. R. *J. Am. Chem. Soc.* **1999**, *121*, 3156.
- (16) Dobado, J. A.; Martínez-García, H.; Molina, J. *Inorg. Chem.* **1999**, *38*, 6257.
- (17) Cioslowski, J.; Surján, P. R. *J. Mol. Struct.* **1992**, *255*, 9.
- (18) El-Bahraoui, J.; Molina, J.; Portal, D. *J. Phys. Chem. A* **1998**, *102*, 2443.
- (19) Dobado, J. A.; Uggla, R.; Sundberg, M. R.; Molina, J. *J. Chem. Soc., Dalton Trans.* **1999**, 489.
- (20) Navarro, J. A. R.; Romero, M. A.; Salas, J. M.; Quiros, M.; El-Bahraoui, J.; Molina, J. *Inorg. Chem.* **1996**, *35*, 7829.
- (21) Bytheway, I.; Gillespie, R. J.; Tang, T.-H.; Bader, R. F. W. *Inorg. Chem.* **1995**, *34*, 2407.
- (22) Gillespie, R. J.; Bytheway, I.; Tang, T.-H.; Bader, R. F. W. *Inorg. Chem.* **1996**, *35*, 3954.
- (23) Frenking, G.; Pidun, U. *J. Chem. Soc., Dalton Trans.* **1997**, 1653.
- (24) Boehme, C.; Uddin, J.; Frenking, G. *Coord. Chem. Rev.*, in press.
- (25) Weiss, J.; Stetzkamp, D.; Nuber, B.; Fischer, R. A.; Boehme, C.; Frenking, G. *Angew. Chem., Int. Ed. Engl.* **1997**, *36*, 70.
- (26) Fischer, R. A.; Schulte, M. M.; Weiss, J.; Zsolnai, L.; Jacobi, A.; Huttner, G.; Frenking, G.; Boehme, C.; Vyboishchikov, S. F. *J. Am. Chem. Soc.* **1998**, *120*, 1237.
- (27) Boehme, C.; Frenking, G. *Chem.—Eur. J.* **1999**, *5*, 2184.

\* Corresponding authors. E-mail addressees: jmolina@ugr.es (for J.M.M.); sundberg@cc.helsinki.fi (for M.R.S.).

- (1) Hückel, E. *Z. Phys.* **1930**, *60*, 423.
- (2) Pauling, L. *J. Am. Chem. Soc.* **1931**, *53*, 1367.
- (3) Slater, J. C. *Phys. Rev.* **1931**, *37*, 481.
- (4) Pauling, L. *Theoretical Organic Chemistry. The Kekule Symposium*; Butterworth: London, 1959.
- (5) Carter, E. A.; Goddard, W. A., III *J. Am. Chem. Soc.* **1988**, *110*, 4077.
- (6) Wiberg, K. B. *Acc. Chem. Res.* **1996**, *29*, 229.
- (7) Dobado, J. A.; Martínez-García, H.; Molina, J.; Sundberg, M. R. *J. Am. Chem. Soc.* **1998**, *120*, 8461.
- (8) Messmer, R. P.; Schultz, P. A. *Chem. Phys. Rev.* **1986**, *57*, 2653.
- (9) Schultz, P. A.; Messmer, R. P. *J. Am. Chem. Soc.* **1993**, *115*, 10925.

**Table 1.** Bond Lengths (Å) and Bond Angles (deg), and Imaginary Frequencies (cm<sup>-1</sup>) for the Titanium<sup>a</sup> (1–4) and Germanium (5–8) Compounds Determined with the 6-311G\* Basis Set

	1, H <sub>3</sub> TiOCH <sub>3</sub>		2, F <sub>3</sub> TiOCH <sub>3</sub>		3 Cl <sub>3</sub> TiOCH <sub>3</sub>		4 Br <sub>3</sub> TiOCH <sub>3</sub>	
	B3LYP	MP2	B3LYP	MP2	B3LYP	MP2	B3LYP	MP2
Ti–O	1.724 (1.724)	1.696 (1.696)	1.740 (1.740)	1.716 (1.716)	1.719 (1.716)	1.696 (1.696)	1.720 (1.720)	1.700 (1.701)
C–O	1.408 (1.408)	1.416 (1.416)	1.404 (1.408)	1.412 (1.412)	1.411 (1.412)	1.420 (1.420)	1.410 (1.412)	1.416 (1.416)
Ti–Y <sup>b</sup>	1.698 (1.698)	1.691 (1.689)	1.756 (1.756)	1.743 (1.743)	2.200 (2.198)	2.162 (2.161)	2.355 (2.355)	2.318 (2.315)
C–H	1.091 (1.091)	1.089 (1.088)	1.092 (1.092)	1.088 (1.090)	1.092 (1.092)	1.090 (1.088)	1.092 (1.090)	1.090 (1.088)
∠O–Ti–Y <sup>b</sup>	106.0 (106.1)	104.7 (104.7)	109.3 (109.3)	109.0 (109.0)	108.1 (108.2)	107.6 (107.7)	107.9 (108.0)	107.3 (107.5)
∠O–C–H	109.5 (109.5)	108.6 (108.7)	109.7 (109.7)	109.1 (109.3)	109.1 (109.3)	108.4 (108.4)	109.1 (109.1)	108.4 (108.7)
imaginary freq	(32i)		46i		39i		50i	

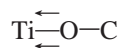
  

	5, H <sub>3</sub> GeOCH <sub>3</sub>		6, F <sub>3</sub> GeOCH <sub>3</sub>		7, Cl <sub>3</sub> GeOCH <sub>3</sub>		8, Br <sub>3</sub> GeOCH <sub>3</sub>	
	B3LYP	MP2	B3LYP	MP2	B3LYP	MP2	B3LYP	MP2
Ge–O	1.793	1.784	1.737	1.727	1.756	1.740	1.763	1.748
C–O	1.417	1.420	1.441	1.437	1.432	1.435	1.432	1.435
Ge–Y <sub>1</sub> <sup>b</sup>	1.532	1.528	1.716	1.704	2.136	2.104	2.300	2.268
Ge–Y <sub>2</sub> <sup>b</sup>	1.545	1.540	1.724	1.713	2.158	2.123	2.324	2.285
C–H <sub>1</sub>	1.093	1.089	1.090	1.087	1.092	1.087	1.092	1.090
C–H <sub>2</sub>	1.095	1.095	1.092	1.090	1.092	1.093	1.093	1.090
∠C–O–Ge	119.5	117.1	121.1	119.3	120.0	119.3	121.9	119.2
∠O–Ge–Y <sub>1</sub> <sup>b</sup>	104.5	104.9	108.8	109.5	106.4	107.4	105.8	106.5
∠O–Ge–Y <sub>2</sub> <sup>b</sup>	109.6	109.5	112.7	112.4	110.0	110.8	110.4	110.4
∠O–C–H <sub>1</sub>	107.6	107.5	105.9	106.1	106.2	106.3	106.3	106.1
∠O–C–H <sub>2</sub>	112.3	111.9	111.3	111.0	111.5	111.2	111.5	111.2
∠Y <sub>1</sub> GeO(Y <sub>2</sub> ) <sup>b</sup>	120.0	120.1	120.1	120.5	120.0	120.4	119.9	120.2
∠H <sub>1</sub> CO(H <sub>2</sub> )	118.8	119.1	118.7	118.8	118.5	118.9	118.8	118.6

<sup>a</sup> Values for the titanium staggered conformation are given in parentheses. <sup>b</sup> Y = H, F, Cl, Br.

recently, a detailed study was performed on the relationship among the  $\pi$  bonding, electronegativity, and geometry of different ligands in early transition metal complexes.<sup>28</sup>

The main goal of this paper is to characterize Ti–O bonding in a series of titanium(IV) methoxides with reference to analogous germanium(IV) complexes. In this context, a series of four-coordinated titanium(IV) alkoxide analogues whose geometries strongly suggest multiple bonding were chosen as model compounds. Indeed, as suggested by Rothwell et al.,<sup>29</sup> the linear (or pseudolinear) Ti–O–C unit could be described as



To investigate the importance of hypovalency (electron deficiency) in Ti(IV) compounds [where the titanium(IV) cation displays an empty outer valence core], we compare them with a series of Ge(IV) complexes (18-electron species). We show the existence of multiple bonding in the Ti(IV) compounds; in contrast, the Ge compounds present only Ge–O single bonds.

## Methods

All calculations were carried out using the Gaussian 98 package<sup>30</sup> of programs. All geometries were fully optimized, and all stationary points on the hypersurface were characterized by harmonic frequency analysis. The B3LYP/6-311G\* and MP2(full)/6-311G\* theoretical levels were used to study all of the compounds (1–8). AIM analyses were performed by the AIMPAC series of programs<sup>31,32</sup> using the B3LYP/

6-311G\* densities as input, as described in the AIM theory.<sup>12–14</sup> The electron localization function (ELF) analysis and the calculation of the electronic densities over the basins were made with the TopMod series of programs.<sup>33</sup> The NLMOs were analyzed using the NBO program<sup>34</sup> within the Gaussian 98 package.<sup>30</sup>

## Results and Discussion

**Geometrical Aspects.** Quantum chemical calculations yielded linear C<sub>3v</sub> geometries for the titanium compounds (1–4) and bent C<sub>s</sub> geometries for the germanium (5–8) compounds (Figure 1). The geometrical data are summarized in Table 1. For compounds 2–4, the eclipsed conformations represent true energy minima and the staggered ones correspond to rotational

(28) Kaupp, M. *Chem.—Eur. J.* **1999**, *5*, 3631.

(29) Coffindaffer, T. W.; Rothwell, I. P.; Huffman, J. C. *Inorg. Chem.* **1983**, *22*, 2906.

- (30) Frisch, M. J.; Trucks, G. W.; Schlegel, H. B.; Scuseria, G. E.; Robb, M. A.; Cheeseman, J. R.; Zakrzewski, V. G., Jr.; Stratmann, R. E.; Burant, J. C.; Dapprich, S.; Millam, J. M.; Daniels, A. D.; Kudin, K. N.; Strain, M. C.; Farkas, O.; Tomasi, J.; Barone, V.; Cossi, M.; Cammi, R.; Mennucci, B.; Pomelli, C.; Adamo, C.; Clifford, S.; Ochterski, J.; Petersson, G. A.; Ayala, P. Y.; Cui, Q.; Morokuma, K.; Malick, D. K.; Rabuck, A. D.; Raghavachari, K.; Foresman, J. B.; Cioslowski, J.; Ortiz, J. V.; Stefanov, B. B.; Liu, G.; Liashenko, A.; Piskorz, P.; Komaromi, I.; Gomperts, R.; Martin, R. L.; Fox, D. J.; Keith, T.; Al-Laham, M. A.; Peng, C. Y.; Nanayakkara, A.; Gonzalez, C.; Challacombe, M.; Gill, P. M. W.; Johnson, B.; Chen, W.; Wong, M. W.; Andres, J. L.; Gonzalez, C.; Head-Gordon, M.; Replogle, E. S.; Pople, J. A.; *Gaussian 98*, Revision A.4; Gaussian, Inc.: Pittsburgh, PA, 1998.
- (31) Biegler-König, F. W.; Bader, R. F. W.; Tang, T. H. *J. Comput. Chem.* **1982**, *3*, 317.
- (32) The AIMPAC package of programs available at [www.chemistry.mcmaster.ca/aimpac](http://www.chemistry.mcmaster.ca/aimpac).
- (33) S. Noury, X. Krokidis, F. Fuster, and B. Silvi, TopMod Package, 1997, available at [www.lct.jussieu.fr/silvi](http://www.lct.jussieu.fr/silvi).
- (34) Glendening, E. D.; Reed, A. E.; Carpenter, J. E.; Weinhold, F. *NBO*, Version 3.1.

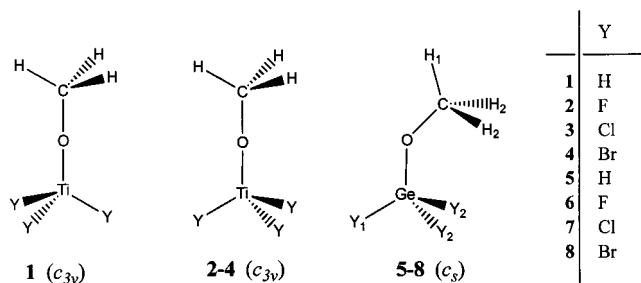
**Table 2.** NBO Analysis of the Titanium (1–4) and Germanium (5–8) Compounds at the B3LYP/6-311G\* Theoretical Level

compd	bond X <sup>a</sup> –O	%X <sup>a</sup> (%s,%p,%d)	%O(%s,%p)	compd	bond X <sup>b</sup> –O	%X <sup>b</sup> (%s,%p)	XO(%s,%p)
<b>1</b> , H <sub>3</sub> TiOCH <sub>3</sub>	Ti–O( $\sigma$ )	12(21,0,79)	88(51,49)	<b>5</b> , H <sub>3</sub> GeOCH <sub>3</sub>	Ge–O( $\sigma$ )	19(23,77)	81(25,75)
	Ti–O( $\pi$ )	9(0,0,100)	91(0,100)		C–O( $\sigma$ )	33(24,76)	67(30,70)
	Ti–O( $\pi$ )	9(0,0,100)	91(0,100)		lone pair1		(44,56)
	C–O( $\sigma$ )	31(22,77,0)	69(49,51)		lone pair2		(0,100)
<b>2</b> , F <sub>3</sub> TiOCH <sub>3</sub>	Ti–O( $\sigma$ )	12(29,0,71)	88(50,50)	<b>6</b> , H <sub>3</sub> GeOCH <sub>3</sub>	Ge–O( $\sigma$ )	18(29,71)	82(19,81)
	Ti–O( $\pi$ )	10(0,0,100)	90(0,100)		C–O( $\sigma$ )	31(22,78)	69(33,67)
	Ti–O( $\pi$ )	10(0,0,100)	90(0,100)		lone pair1		(48,52)
	C–O( $\sigma$ )	31(23,77,0)	69(50,50)		lone pair2		(0,100)
<b>3</b> , Cl <sub>3</sub> TiOCH <sub>3</sub>	Ti–O( $\sigma$ )	14(23,0,77)	86(51,49)	<b>7</b> , Cl <sub>3</sub> GeOCH <sub>3</sub>	Ge–O( $\sigma$ )	19(29,71)	81(23,77)
	Ti–O( $\pi$ )	12(0,0,100)	88(0,100)		C–O( $\sigma$ )	31(22,78)	69(31,69)
	Ti–O( $\pi$ )	12(0,0,100)	88(0,100)		lone pair1		(46,54)
	C–O( $\sigma$ )	30(22,78,0)	70(49,51)		lone pair2		(0,100)
<b>4</b> , Br <sub>3</sub> TiOCH <sub>3</sub>	Ti–O( $\sigma$ )	14(22,0,78)	86(51,49)	<b>8</b> , Br <sub>3</sub> GeOCH <sub>3</sub>	Ge–O( $\sigma$ )	19(29,71)	81(23,77)
	Ti–O( $\pi$ )	12(0,0,100)	88(0,100)		C–O( $\sigma$ )	31(22,78)	69(31,69)
	Ti–O( $\pi$ )	12(0,0,100)	88(0,100)		lone pair1		(46,54)
	C–O( $\sigma$ )	30(22,78,0)	70(49,51)		lone pair2		(0,100)

<sup>a</sup> X = C, Ti. <sup>b</sup> X = C, Ge.

**Table 3.** Charge Densities,  $\rho(r)$ , Laplacians of the Charge Densities,  $\nabla^2\rho(r)$ , and Local Energy Densities,  $E_d(r)$ , for the BCPs of the Titanium (1–4) and Germanium (5–8) Compounds at the B3LYP/6-311G\* Theoretical Level

compd		$\rho(r)$ e/a <sub>0</sub> <sup>3</sup>	$\nabla^2\rho(r)$ e/a <sub>0</sub> <sup>5</sup>	$ \lambda_1/\lambda_3 $	$E_d(r)$ hartree/a <sub>0</sub> <sup>3</sup>	compd		$\rho(r)$ e/a <sub>0</sub> <sup>3</sup>	$\nabla^2\rho(r)$ e/a <sub>0</sub> <sup>5</sup>	$ \lambda_1/\lambda_3 $	$E_d(r)$ hartree/a <sub>0</sub> <sup>3</sup>
<b>1</b>	Ti–O	0.167	0.885	0.192	–0.063	<b>5</b>	Ge–O	0.134	0.526	0.223	–0.050
	O–C	0.243	–0.230	0.696	–0.319		O–C	0.252	–0.446	0.989	–0.322
	Ti–H	0.106	–0.031	0.545	–0.049		Ge–H <sub>1</sub>	0.131	–0.019	0.533	–0.081
<b>2</b>	Ti–O	0.160	0.849	0.188	–0.058	<b>6</b>	Ge–O	0.155	0.641	0.224	–0.065
	O–C	0.244	–0.219	0.697	–0.320		O–C	0.231	–0.318	0.870	–0.286
	Ti–F	0.156	0.822	0.211	–0.042		Ge–F <sub>1</sub>	0.144	0.802	0.188	–0.039
<b>3</b>	Ti–O	0.172	0.890	0.195	–0.069	<b>7</b>	Ge–O	0.149	0.598	0.224	–0.060
	O–C	0.238	–0.157	0.630	–0.311		O–C	0.235	–0.331	0.875	–0.294
	Ti–Cl	0.098	0.208	0.278	–0.033		Ge–Cl <sub>1</sub>	0.107	0.099	0.353	–0.052
<b>4</b>	Ti–O	0.171	0.886	0.195	–0.068	<b>8</b>	Ge–O	0.145	0.574	0.225	–0.058
	O–C	0.239	–0.164	0.635	–0.312		O–C	0.237	–0.341	0.883	–0.297
	Ti–Br	0.084	0.135	0.296	–0.027		Ge–Br <sub>1</sub>	0.094	0.024	0.444	–0.043

**Figure 1.** The titanium (1–4) and germanium (5–8) compounds.

transition states. For **1**, the staggered conformation is the minimum. Compounds **1–4** present a negligible barrier to rotation about the C<sub>3</sub> axis. Moreover, the imaginary frequencies are very low, so that the energies for the transition states and minima are very close in magnitude. This is especially true for compound **1**, in which the energy difference is only 0.06 kcal/mol at the MP2(full)/6-311G\* level. Also, the overall geometrical parameters (bonds, angles) are very similar (see Table 1). The different natures of the substituents (H, F, Cl, Br) on the titanium compounds (**1–4**) have a noticeable influence not only on the Ti–Y bonds but also on the Ti–O bond and, to a slight degree, on the C–O bond. The Ti–O bond lengthens when the electronegativities of the substituents on Ti increase, with the result that there is a marked difference between compound **2** (Y = F) and the other titanium compounds (see Table 1). This difference could be also explained by fluorine  $\pi$  donation to the Ti atom, in agreement with the influence of the substituent  $\pi$ -bonding in the geometry of high-valent transition metal complexes proposed by Kaupp.<sup>28</sup> The effect on the C–O

bond is small and is in the opposite direction. The Ti–O bond lengthens when highly electronegative substituents are attached to Ti with a d<sup>10</sup> electronic configuration. Compound **2** has the shortest C–O bond. The germanium compounds (**5–8**) exhibit  $\angle\text{Ge–O–C}$  angles of about 120°. The Ge–O bond length is close to the length of the average Ge–O single bond, and the influence of substituents is opposite to that in the titanium compounds. The Ge–O bond length decreases as the electronegativities of the substituents increase, giving lengths in the order **5** < **8** < **7** < **6** (see Table 1). The C–O bond lengthens with the electronegativities of the substituents (in opposition to the Ge–O bond), giving always larger values than those for the C–O bond lengths in the titanium compounds. As a test of the reliability of the DFT results, Table 1 compares the DFT data with the MP2 data. The results of the two methods are in good agreement, though Ti–O and Ge–O bond lengths are shorter and C–O bond lengths are longer at the MP2 level.

The geometrical data strongly suggest multiple bonding for the linear titanium alkoxide complexes and single Ge–O bonds for the germanium alkoxide complexes.

**Electronic Properties.** The overall electronic picture of the titanium and germanium compounds was evaluated by NBO methods, AIM theory, and ELF topology analyses. The numerical results are presented in Tables 2–6. The multiple-bonding nature identified in the titanium alkoxide compounds and not in the germanium alkoxide compounds is clearly seen in the results of the electronic analyses.

The results obtained with the NBO methods are given in Table 2, in which the NLMO values are summarized. The multiple bonding in the titanium compounds (**1–4**) unmistakably

**Table 4.** Electron Charge Densities,  $\rho(r)$ , Laplacians of the Charge Densities,  $\nabla^2\rho(r)$ , and Geometrical Dispositions for the Maxima on  $-\nabla^2\rho(r)$  in the Ge, Ti, and O Atoms at the B3LYP/6-311G\* Theoretical Level

	maxima	$\rho(r)$ (e/a <sub>0</sub> <sup>3</sup> )	$\nabla^2\rho(r)$ (e/a <sub>0</sub> <sup>5</sup> )	dist (Å) <sup>a</sup>		maxima	$\rho(r)$ (e/a <sub>0</sub> <sup>3</sup> )	$\nabla^2\rho(r)$ (e/a <sub>0</sub> <sup>5</sup> )	dist (Å) <sup>a</sup>
1 at Ti		1.446	-12.215	0.406	5 at Ge		10.165	-140.668	0.249
		1.512	-14.671	0.402		<i>b</i>	10.157	-140.270	0.249
		1.501	-14.518	0.402			10.113	-137.946	0.250
		1.548	-15.139	0.401					
1 at O	<i>c</i>	0.862	-3.862	0.352	5 at O	<i>b</i>	0.937	-4.820	0.343
		0.696	-2.371	0.379			0.672	-2.045	0.384
2 at Ti		1.403	-11.794	0.407	6 at Ge		10.130	-138.352	0.250
		1.420	-11.441	0.407		<i>b</i>	10.121	-137.869	0.250
		1.377	-11.469	0.407			10.193	-140.771	0.249
		1.447	-12.350	0.406					
2 at O	<i>c</i>	0.864	-3.867	0.351	6 at O	<i>b</i>	0.938	-4.831	0.343
		0.691	-2.278	0.380			0.686	-2.195	0.380
3 at Ti		1.408	-11.671	0.407	7 at Ge		10.172	-139.753	0.249
		1.400	-11.573	0.407		<i>b</i>	10.072	-136.040	0.250
		1.430	-11.951	0.407			10.084	-136.607	0.250
		1.385	-10.781	0.409					
3 at O	<i>c</i>	0.859	-3.844	0.352	7 at O	<i>b</i>	0.936	-4.815	0.343
		0.703	-2.440	0.378			0.686	-2.205	0.380
4 at Ti		1.406	-11.607	0.407	8 at Ge		10.070	-136.059	0.250
		1.423	-11.826	0.407		<i>b</i>	10.058	-135.470	0.250
		1.401	-11.553	0.407			10.160	-139.272	0.250
		1.377	-10.664	0.409					
4 at O	<i>c</i>	0.859	-3.845	0.352	8 at O	<i>b</i>	0.935	-4.806	0.343
		0.703	-2.442	0.378			0.686	-2.205	0.380

<sup>a</sup> Distance from the maximum to its corresponding atom. <sup>b</sup> This maximum has an additional equivalent one. <sup>c</sup> This maximum has two additional equivalent ones.

**Table 5.** AIM and NBO (in Parentheses) Atomic Charges and Delocalization Indices,  $\delta(\text{Ti},\text{O})$  and  $\delta(\text{Ge},\text{O})$ , for the Titanium (1–4) and Germanium (5–8) Compounds at the B3LYP/6-311G\* Theoretical Level

	1	2	3	4		5	6	7	8
at Ti	1.82 (1.44)	2.29 (1.89)	1.94 (1.38)	1.87 (1.35)	at Ge	1.55 (1.00)	2.47 (2.33)	1.90 (1.49)	1.67 (1.26)
at O	-1.08 (-0.70)	-1.09 (-0.71)	-1.05 (-0.62)	-1.06 (-0.63)	at O	-1.12 (-0.84)	-1.08 (-0.88)	-1.09 (-0.85)	-1.09 (-0.85)
at Y <sup>a</sup>	-0.45 (-0.36)	-0.61 (-0.51)	-0.51 (-0.38)	-0.49 (-0.36)	at Y <sub>1</sub> <sup>a</sup>	-0.30 (-0.13)	-0.65 (-0.59)	-0.45 (-0.31)	-0.36 (-0.23)
					at Y <sub>2</sub> <sup>a</sup>	-0.32 (-0.16)	-0.65 (-0.60)	-0.46 (-0.33)	-0.39 (-0.26)
at C	0.44 (-0.17)	0.45 (-0.17)	0.43 (-0.17)	0.43 (-0.17)	at C	0.44 (-0.17)	0.39 (-0.17)	0.39 (-0.18)	0.40 (-0.18)
at H	0.06 (0.17)	0.05 (0.17)	0.07 (0.18)	0.07 (0.18)	at H <sub>1</sub>	0.04 (0.17)	0.07 (0.18)	0.07 (0.18)	0.06 (0.18)
					at H <sub>2</sub>	0.01 (0.15)	0.03 (0.17)	0.05 (0.17)	0.04 (0.16)
at OCH <sub>3</sub>	-0.46 (-0.36)	-0.49 (-0.37)	-0.41 (-0.25)	-0.42 (-0.27)	at OCH <sub>3</sub>	-0.62 (-0.54)	-0.56 (-0.53)	-0.53 (-0.51)	-0.55 (-0.53)
$\delta(\text{Ti},\text{O})$	1.07	0.96	1.08	1.08	$\delta(\text{Ge},\text{O})$	0.76	0.77	0.78	0.79

<sup>a</sup> Y = H, F, Cl, Br.

shows the characteristics of a triple bond as described in the Hückel model. Three bonding molecular orbitals (MOs) are observed, each displaying clear ionic character. As expected, one MO is a  $\sigma$  Ti–O bond formed between an sp atomic orbital (AO) of oxygen and the empty sd<sup>3</sup> hybridized AO of titanium. The two remaining MOs display  $\pi$  character with interaction between the empty d AOs of Ti and the occupied p orbitals of O. In every compound, the C–O bond appears as a normal single  $\sigma$  bond.

The Ge–O bond in compounds 5–8 is totally different. The NBO analyses show only one MO, again of a very ionic character. The MO is formed by sp<sup>3</sup> AOs of Ge and O. There are also two additional electron lone pairs for oxygen. The C–O bonds clearly exhibit single- $\sigma$ -bond character.

The results obtained by the AIM method are collected in Tables 3–5 and illustrated in Figure 2. The numerical values of the bond critical points (BCPs) in  $\rho(r)$  imply stronger bonds for Ti–O than for Ge–O (see Table 3). In both series, the

metal–oxygen bonds are of closed-shell interaction type (highly polarized character). However, a small covalent character is proposed on the basis of the negative electron energy density values. This is also corroborated for the  $|\lambda_1/\lambda_3|$  values in the Ti–O bond critical points (values of ca. 0.19 compared with ca. 0.15 for alkali metal halides<sup>35</sup>). The geometrical effects associated with the metal substituents (see above) can be rationalized in terms of the numerical values of the bond critical points in  $\rho(r)$ . Both single and triple bonds are compatible with the numerical bond critical point data. However, a different representation is obtained in the  $\nabla^2\rho(r)$  topology study. The numerical data summarized in Table 4 give the electron density concentration maxima surrounding the metal and oxygen for compounds 1–8. For the titanium compounds, four maxima are located on oxygen, one of them on the C<sub>3</sub> symmetry axis toward the carbon atom and the three additional ones in a plane

(35) See ref 12, p 291.



**Table 6.** ELF Analysis Including Basins, Populations, and Cross-Exchange Contributions of the Core Metal Basins, for Compounds **1** and **5** at the B3LYP/6-311G\* Theoretical Level

1			5		
basins <sup>a</sup>	pop.	cross-exchange contribns	basins <sup>a</sup>	pop.	cross-exchange contribns
C(Ti)	19.29		C(Ge)	27.74	
V(Ti,H)	1.70	0.33	V(Ge,H <sub>1</sub> )	2.12	0.29
			V(Ge,H <sub>2</sub> )	2.12	0.28
			V(Ge,O)	0.60	0.05
C(O)	2.16	0.02	C(O)	2.13	0.00
V(O)	5.93	0.41	V <sub>1</sub> (O)	2.85	0.06
			V <sub>2</sub> (O)	2.84	0.06
V(O,C)	1.32	0.03	V(O,C)	1.23	0.00
C(C)	2.09	0.00	C(C)	2.09	0.00
V(C,H)	2.03	0.01	V(C,H <sub>1</sub> )	2.04	0.00
			V(C,H <sub>2</sub> )	2.05	0.00

<sup>a</sup> C corresponds to core and V to valence.

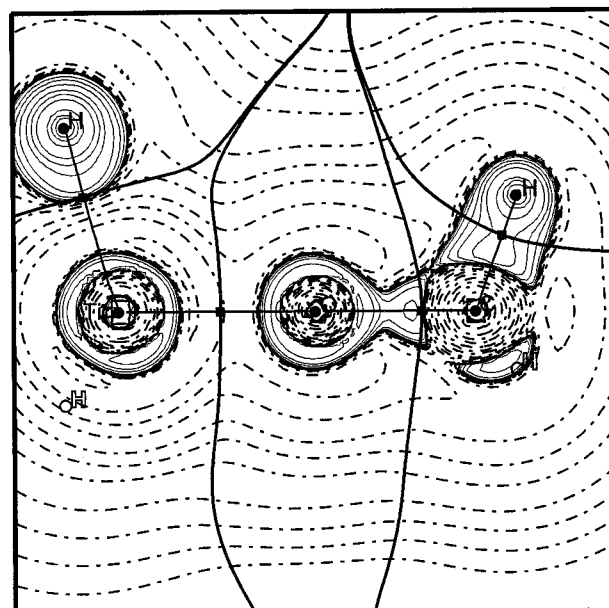
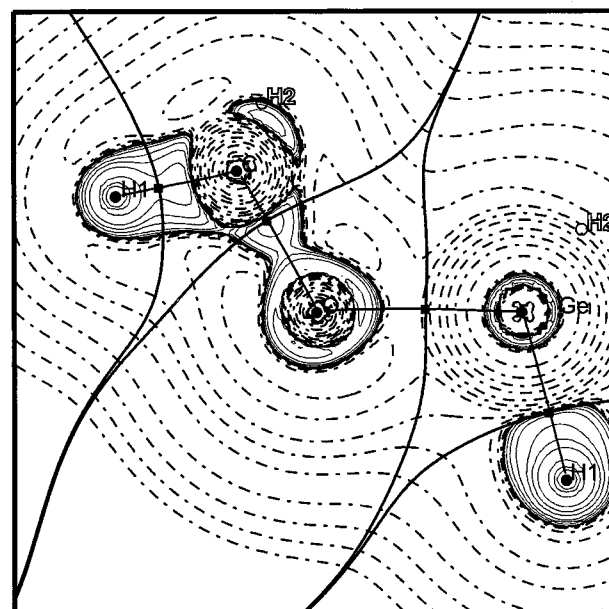
perpendicular to the C<sub>3</sub> symmetry axis toward the Ti atom. There are also four maxima for the Ge compounds, two of them on the C–O and Ge–O bonds and two compatible with a two-electron pair at oxygen atom. The features described above are depicted in Figure 2.

For the titanium compounds (**1–4**), the description of the electron charge concentration surrounding the oxygen and directed toward the Ti atom, together with the one single maximum in the C–O bond, favors a triple bond. The description of the Ge–O bond, on the other hand, matches that of a standard single bond. No doubt, the triple-bond formation for the titanium compounds is due to hypovalency. In addition, four inner electron concentration maxima were found in the titanium atom environment, directed away from the four ligands bonded to titanium. These maxima were associated with the titanium third shell (the core distortion was first noted by Bader).<sup>21,22,36</sup> The charges on the metal atoms indicate an electron donation from the ligand (see Table 5). All the charges lie in the same range. A higher electron donation was observed from the methoxide group to titanium than to germanium (with methoxide group charges of ca. –0.45 for the Ti compounds in comparison with ca. –0.57 for the Ge compounds). The larger stabilization in the titanium series due to higher electron donation is also reflected in the charge differences between the Ti atoms in **1** and **2**, increased by 0.47 compared with **5** and **6** when the H atoms are replaced by F ones.

The quantum mechanical pair density, in conjunction with the quantum definition of an atom in a molecule, provides a precise determination of the extent to which electrons are localized in a given atom and delocalized over any pair of atoms.<sup>37</sup> The electron pairing is a consequence of the Pauli exclusion principle, and the extent of spatial localization of the pairing is determined by the corresponding property of the Fermi hole density. These ideas are made quantitative through the appropriate integration of the pair density to determine the total Fermi correlation contained within a single atomic basin,  $F(A,A)$ , or the correlation shared between two basins,  $F(A,B)$ . The quantity  $F(A,B)$  is thus a measure of the extent to which electrons of either spin referenced to atom A are delocalized onto atom B with a corresponding definition of  $F(B,A)$ . Thus,

(36) This core distortion has been discussed for the TiCl<sub>2</sub>Me<sub>2</sub> structure by considering the similar geometrical descriptions for these compounds using all-electron basis sets and 18-electron effective core potentials: Bader, R. F. W.; Gillespie, R. J.; Marin, F. *Chem. Phys. Lett.* **1998**, *290*, 488.

(37) Fradera, X.; Austen, M. A.; Bader, R. F. W. *J. Phys. Chem. A* **1999**, *103*, 304.

**1****5**

**Figure 2.** Laplacian of  $\rho(r)$  contour maps, in the molecular plane obtained using the MORPHY98 program,<sup>41</sup> for structures **1** and **5** at the B3LYP/6-311G\* theoretical level. The contours begin at zero and increase (solid contours) and decrease (dashed contours) in steps of  $\pm 0.02$ ,  $\pm 0.04$ ,  $\pm 0.08$ ,  $\pm 0.2$ ,  $\pm 0.4$ ,  $\pm 0.8$ ,  $\pm 2.0$ ,  $\pm 4.0$ , and  $\pm 8.0$ . The thick solid lines represent the molecular graph that joins the nuclei (solid circles) and the BCP (solid squares) and also represent the zero-flux surface.

$F(B,A) = F(A,B)$  and their sum,  $F(A,B) + F(B,A) = \delta(A,B)$ , termed the delocalization index, is a measure of the total Fermi correlation shared between the atoms. This delocalization index is formulated by taking into account

$$F(A,B) = F(B,A) = - \sum_i \sum_j S_{ij}(A) S_{ij}(B)$$

where  $S_{ij}(A)$  is the corresponding atomic overlap matrix given by the PROAIM program.<sup>31</sup> The calculated  $\delta(\text{Ti},\text{O})$  and  $\delta(\text{Ge},\text{O})$  values for compounds **1–8** are listed in Table 5. The  $\delta(\text{Ti},\text{O})$

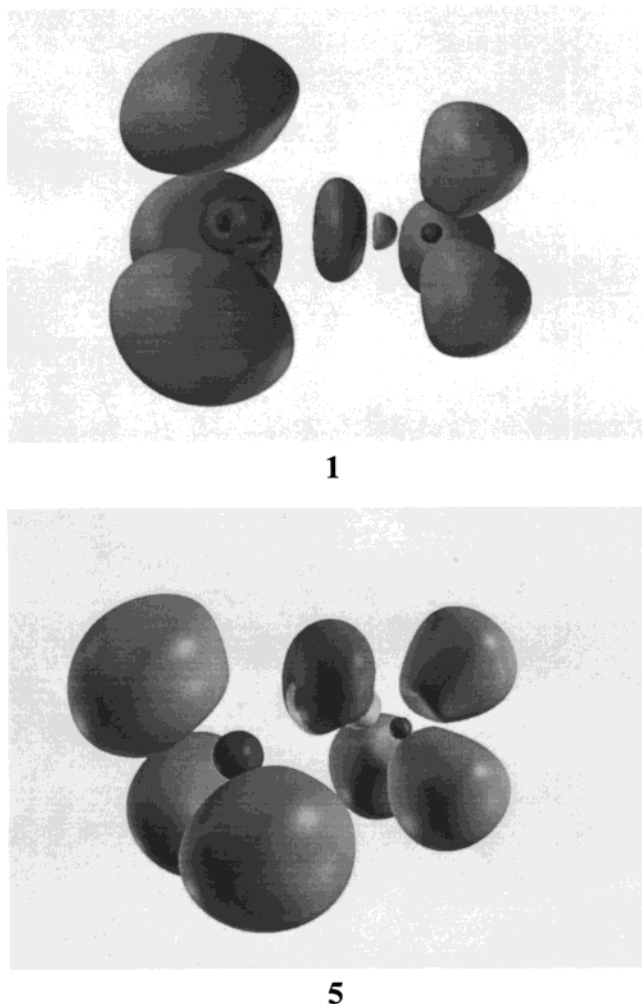


**Figure 3.** ELF isosurface plots (0.8 and 0.75) for structures **1** and **5** at the B3LYP/6-311G\* theoretical level.

values are considerably higher than the corresponding  $\delta(\text{Ge},\text{O})$  values (ca. 1.0 and 0.7 electron pair, respectively). Taking into account the very polarized nature<sup>38</sup> of the bonds, the values are consistent with Ti–O multiple bonds and with noticeable covalent character.

(38) The formal  $\delta$  value for a pure ionic bond is zero.

The ELF has proven to be effective tool in studying chemical bonds.<sup>39</sup> Data for compounds **1** and **5** are collected in Table 6, and ELF plots are shown in Figure 3. For compound **1**, two valence basins were found on the O atom, one disynaptic and the other one monosynaptic.<sup>40</sup> The population of the monosynaptic basin is close to 6 electrons, corresponding to the three electron pairs on oxygen. This basin has a semispherical shape, rounding the O atom and situated toward the Ti core (see Figure 3), characteristic of a triple bond, though a very polarized one. In addition, the cross-exchange between the Ti core basin,  $C(\text{Ti})$ , and the O monosynaptic valence basin,  $V(\text{O})$ , is large, even larger than that for the valence titanium hydrogen basins,  $V(\text{Ti},\text{H})$  (see Table 6). This indicates a net electronic exchange between the electron pair on O and the Ti atom.

On the other hand, compound **5** displays four valence basins on the oxygen atom, two of them disynaptic ( $V(\text{Ge},\text{O})$  and  $V(\text{O},\text{C})$ ), corresponding to the Ge–O and O–C bonds. The two remaining monosynaptic  $V(\text{O})$  basins belong to the other electron pairs on the O atom. The above valence basin distribution corresponds to a bent Ge–O–C geometry (see Figure 3). This represents a standard Ge–O single bond. In addition, the cross-exchange between the Ge core,  $C(\text{Ge})$ , and the oxygen valence,  $V(\text{O})$ , basins is very small, indicating a low stabilization of the Ge charge by the methoxide group.

**Conclusions.** The linear disposition of  $\angle\text{Ti–O–C}$  angles in the series of titanium alkoxides (**1–4**) has been rationalized by a polarized triple Ti–O bond, on the basis of electronic analyses including NBO, ELF, AIM, and electron delocalization indexes. On the other hand, the 18-electron germanium series of compounds (**5–8**) presented bent  $\angle\text{Ge–O–C}$  angles compatible with a standard single Ge–O bond, with two additional electron lone pairs on the oxygen atom.

**Acknowledgment.** Computing time was provided by the Centre of Scientific Computing, Espoo, Finland, and the University of Granada. We are grateful to professor R. F. W. Bader for a copy of the AIMPAC package of programs.

IC000013D

(39) Silvi, B.; Savin, A. *Nature* **1994**, *371*, 683.

(40) The valence basins are characterized by their synaptic order which is the number of core basins with which they share a common boundary. Accordingly, a basin may be mono-, di-, or polysynaptic corresponding to a lone pair, bicentric, or polycentric bonding region, respectively. See: Savin, A.; Silvi, B.; Colonna, F. *Can. J. Chem.* **1996**, *74*, 1088.

(41) MORPHY98 is a program written by P. L. A. Popelier with a contribution from R. G. A. Bone, UMIST, Manchester, England, 1998.